Article

Crystal Structure and Anti-Proliferative and Mutagenic Evaluation of the Palladium(II) Complex of Deoxyalliin

Tuany Zambroti Candido [1], Mariana Mazzo Quintanilha [2,3], Bianca Alves Schimitd [2,3], Déborah de Alencar Simoni [2], Douglas Hideki Nakahata [4], Raphael Enoque Ferraz de Paiva [4], Igor Henrique Cerqueira [5], Flávia Aparecida Resende [5], João Ernesto Carvalho [3], Ana Lucia Tasca Gois Ruiz [3], Carmen Silvia Passos Lima [1,*] and Pedro Paulo Corbi [2,*]

1   Department of Anesthesiology, Oncology and Radiology, Faculty of Medical Sciences, University of Campinas (UNICAMP), Campinas 13083-887, SP, Brazil; tuanyzcandido@gmail.com
2   Institute of Chemistry, University of Campinas (UNICAMP), Campinas 13083-970, SP, Brazil; mariana.mquintanilha@gmail.com (M.M.Q.); schimitdbianca@gmail.com (B.A.S.); dsimoni@unicamp.br (D.d.A.S.)
3   Faculty of Pharmaceutical Sciences, University of Campinas (UNICAMP), Campinas 13083-871, SP, Brazil; carvalho@fcf.unicamp.br (J.E.C.); ana.ruiz@fcf.unicamp.br (A.L.T.G.R.)
4   Donostia International Physics Center (DIPC), Donostia, 20018 Gipuzkoa, Spain; douglas.nakahata@dipc.org (D.H.N.); raphael.depaiva@dipc.org (R.E.F.d.P.)
5   Department of Biological and Health Sciences, University of Araraquara (UNIARA), Araraquara 14801-340, SP, Brazil; ihcerqueira@uniara.edu.br (I.H.C.); farnogueira@uniara.edu.br (F.A.R.)
*   Correspondence: ppcorbi@unicamp.br (P.P.C.); carmenl@fcm.unicamp.br (C.S.P.L.); Tel.: +55-193-521-3130 (P.P.C.)

Abstract: Platinum(II) and palladium(II) complexes have been investigated as potential anticancer drugs since the serendipitous discovery of the antineoplastic activities of cisplatin in the 1960s. Skin cancer is considered the most common malignant neoplasm that affects humans, and melanoma is the most lethal type of skin cancer. Surgical excision is the main form of treatment, which also may include radiotherapy, systemic chemotherapy, and immunotherapy. In this work, new insights concerning the structural characterization and in vitro anti-proliferative activity of the palladium(II) complex with the amino acid deoxyalliin (Pd-sac) against a panel of thirteen human tumor cells, with emphasis on skin cancer cell lines, are presented. The composition of the complex was confirmed by elemental analysis as $[Pd(C_6H_{10}NO_2S)_2]$. The structure of the complex was elucidated for the first time by a single-crystal X-ray diffraction technique. Each deoxyalliin molecule coordinates in a bidentate N,S-mode to palladium(II) in a *trans*-configuration analogous to the platinum(II) deoxyalliin complex early reported. As the main result, the Pd-sac complex showed a selective anti-proliferative activity against melanoma (UACC-62, TGI = 63.5 μM), while both deoxyalliin and K_2PdCl_4 were inactive against all cell lines. Moreover, Pd-sac did not affect the proliferation of non-tumorigenic keratinocytes (HaCaT, TGI > 586 μM) and was non-mutagenic in the Ames assay. The results open new perspectives for in vivo studies concerning the application of the Pd-sac complex in the treatment of melanoma.

Keywords: palladium(II); deoxyalliin; crystal structure; squamous cell carcinoma; melanoma

1. Introduction

Metals were used empirically for centuries in the treatment of several human conditions. Some of the first reports date to 2500 BC, when gold and silver were used in the preparation of magical or mystical potions for the treatment of diseases [1–3]. One of the first reports of the rational use of metals in medicine refers to the preparation of iron solutions for the treatment of anemia in the 8th century, but only at the end of the 1890s did Robert Kock use a well-defined compound, $K[Au(CN)_2]$, as an antibacterial agent for the treatment of tuberculosis [3].

The serendipitous discovery of the anti-proliferative activity of cisplatin, or *cis*-diamminedichoridoplatinum(II), over tumor cells in the 1960s is considered a milestone in the development of modern medicinal inorganic chemistry and the rational use of metals in medicine [4]. Today, cisplatin, carboplatin, and oxaliplatin are platinum(II)-based complexes applied worldwide for the treatment of ovarian, head and neck, and testicular cancers, among others [5–7]. After the discovery of the activity of platinum(II) compounds for cancer treatment, new metal-based compounds were investigated for the same purposes. In this sense, ruthenium(II/III), copper(I/II), iridium(I), rhenium(I), and palladium(II) are examples of some considered metal ions for the synthesis of new candidates as antineoplastic agents [8].

Specifically, palladium(II) complexes have been studied in the search for new anticancer drugs due to the similarity of this metal ion with platinum(II). Both metals present the same coordination modes and form square-planar complexes with similar ligands [9,10]. Additionally, their complexes have been shown to possess anti-proliferative activities over prokaryotic and eukaryotic cells [11]. Recently, the palladium(II) complex padeliporfin (sold under the brand Tookad® Soluble) became the first palladium(II) complex approved for clinical use in the EU [12]. This water-soluble complex is indicated for vascular-targeted photochemotherapy of low-risk prostate cancer [13].

Squamous cell carcinoma (SCC) develops from the stem cells of the basal cell layer of the epidermis. Cutaneous SCC accounts for around 20% of all cases of keratinocyte carcinomas, the most prevalent type of cancer in the population of European descent [14]. Melanoma arises from genetic mutations in the melanocyte progenitor cells. Although it accounts for only 1% of all skin malignant tumors diagnosed, it is the deadliest and most aggressive [14]. The first line of treatment for SCC and melanoma patients is surgery. Immunotherapy has been indicated for both SCC (cemiplimab) and melanoma (ipilimumab, pembrolizumab [15], and nivolumab [16]). Cisplatin can be administered off-label in melanoma treatment regimens [17,18], and palladium(II) complexes emerge as promising agents against melanoma [19–22] from the viewpoint of potency and selectivity for skin cancer [23].

In a recent work, our research group described a silver-based complex that shows in vitro and in vivo anti-proliferative effects over skin SCC. Obtained by the reaction of silver nitrate and the anti-inflammatory nimesulide (NMS), the Ag-NMS complex exhibited important anti-proliferative activities in vitro against SCC15 and FaDu SCC lines (TGI = 67.3 and 107.3 μM, respectively) [24]. In an in vivo skin SCC model in mice induced by 7,12-dimethylbenzanthracene/12-o-tetradecanoyl-phorbol-13-acetate (DMBA/TPA), the complex was able to reduce tumor size up to 100% when applied topically for 21 days, and no toxicity was observed [24].

Our group has been exploring S-allyl-L-cysteine (sac, L-deoxyalliin; Figure 1) as a ligand-seeking antitumor agent over the past two decades. The first reports of the synthesis and anti-proliferative activities over tumor cells of the palladium(II) complex of sac (Pd-sac) were made by us in 2005 [25,26]. At that time, in vitro testing revealed that the complex was able to completely inhibit HeLa (human cervix cancer) cell proliferation and reduce TM5 (murine melanoma) cell proliferation by 75% at a concentration of 0.40 mM. In the sequence, the most probable structure of the complex was described based on a combination of solid-state nuclear magnetic spectroscopic data and DFT studies [27] since no crystals were obtained for a detailed structural determination at the time.

In this work, we present for the first time the structural characterization of the Pd-sac complex based on single-crystal X-ray crystallographic determination, along with the evaluation of its anti-proliferative activity over a panel of human tumorigenic cell lines and its mutagenic effects in the Ames assay.
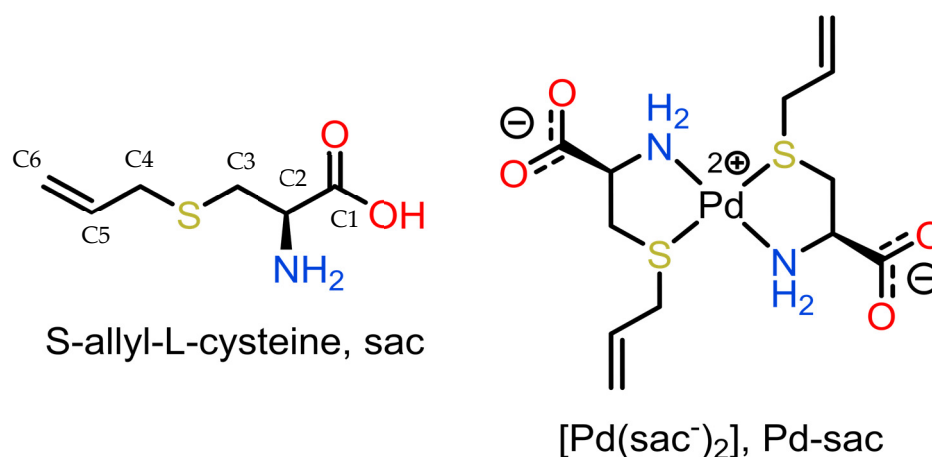
Figure 1. Representation of S-allyl-L-cysteine (sac; deoxyalliin) and its Pd(II) complex.

2. Results

2.1. Structural Commentary and Supramolecular Features

The Pd-sac complex crystallized in the monoclinic C2 space group. The structure of Pd-sac presents square-planar geometry around the Pd atom, with N,S-bidentate coordination of two sac ligands in *trans* configuration (Figure 2). The Pd atom is located in a special position over a 2-fold axis so that the asymmetric unit consists of only one ligand coordinated to Pd(II). The carboxylate groups are deprotonated, balancing the charge from Pd(II). The Pd−N and Pd−S bond lengths are 2.042(3) Å and 2.2975(8) Å (Table 1), respectively.
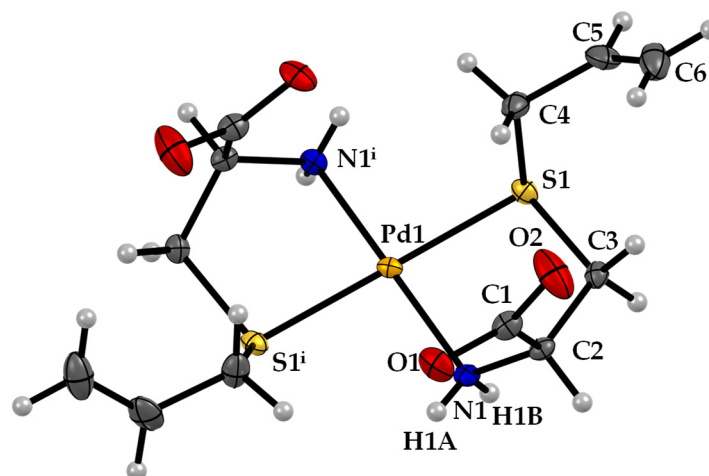
Figure 2. ORTEP diagram, including atom labeling of the Pd-sac structure. Anisotropic displacement ellipsoids are drawn at the 50% probability level.

Table 1. Main bond lengths (Å) and angles (°) for Pd-sac.

Bond Lengths (Å)			
Pd1—N1 [i]	2.042 (3)	N1—C2	1.478 (6)
Pd1—N1	2.042 (3)	N1—H1A	0.80 (4)
Pd1—S1[i]	2.2975 (8)	N1—H1B	0.88 (5)
Pd1—S1	2.2975 (8)	C1—C2	1.533 (5)
S1—C3	1.822 (4)	C2—C3	1.520 (5)
S1—C4	1.829 (5)	C4—C5	1.485 (6)
O1—C1	1.255 (5)	C5—C6	1.318 (8)
O2—C1	1.228 (5)		

Table 1. *Cont.*

Bond Angles (°)			
N1^i—Pd1—N1	176.6 (4)	C2—N1—H1B	109 (3)
N1^i—Pd1—S1 ^{i}	84.30 (9)	Pd1—N1—H1B	102 (3)
N1—Pd1—S1 ^{i}	95.73 (9)	H1A—N1—H1B	115 (5)
N1^i—Pd1—S1	95.73 (9)	O2—C1—O1	126.1 (4)
N1—Pd1—S1	84.30 (9)	O2—C1—C2	117.1 (4)
S1^i—Pd1—S1	179.08 (12)	O1—C1—C2	116.7 (4)
C3—S1—C4	101.6 (2)	N1—C2—C3	109.3 (3)
C3—S1—Pd1	99.81 (12)	N1—C2—C1	111.1 (4)
C4—S1—Pd1	105.60 (16)	C3—C2—C1	114.7 (3)
C2—N1—Pd1	111.9 (3)	C2—C3—S1	111.7 (3)
C2—N1—H1A	109 (3)	C5—C4—S1	109.2 (3)
Pd1—N1—H1A	110 (3)	C6—C5—C4	122.9 (5)

Symmetry code: (i) $-x + 1, y, -z + 1$.

The supramolecular structure of Pd-sac is mainly formed by hydrogen bonding between the amine groups and the anionic carboxylates (Table S1). Specifically, the N1-H1B···O1^{ii} and N1-H1B···O2^{ii} bifurcated hydrogen bond contributes to lattice growth along the *b*-axis, with stacking of the molecules considering the coordination plane (distance between Pd(II) centers of 5.6 Å). Meanwhile, the N1—H1*A*···O1^i hydrogen bond contributes to lattice expansion along the *a*-axis (Figure 3).
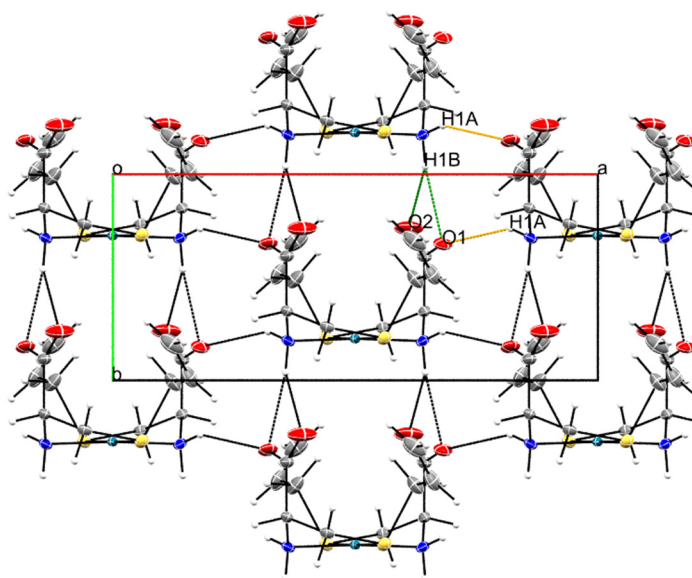

Figure 3. Packing observed in the crystal structure Pd-sac as observed along the crystallographic c-axis. The orange dashed line represents N1—H1*A*···O1^i hydrogen bonds, while the green ones represent N1—H1*B*···O1^{ii} and N1—H1*B*···O2^{ii}. Symmetry codes: (i) $-x + 3/2, y + 1/2, -z + 1$; (ii) $x, y + 1, z$ (see Table S1).

2.2. Anti-Proliferative Activity

Both deoxyalliin and the palladium(II) salt were inactive against all evaluated cell lines (Figure S2, Table 2). Doxorubicin was used as an experimental control to evidence the differential responses of the tested cell lines (Figure S3b,d, Table 2). Expressed as the concentration required to elicit total cell growth inhibition (TGI), the Pd-sac complex exhibited modest but selective activity (Figure S3a,c) against melanoma (UACC-62, TGI = 63.5 µmol L^{-1}) and prostatic adenocarcinoma (PC-3, TGI = 155.6 µmol L^{-1}) (Table 2). Moreover, Pd-sac did not significantly affect the proliferation of non-tumorigenic keratinocytes (HaCaT, TGI > 500 µmol L^{-1}).

Table 2. Anti-proliferative activity of Pd-sac complex; doxorubicin (the reference chemotherapeutical agent), deoxyalliin (sac), and palladium(II) salt expressed as concentration required to completely inhibit proliferation (TGI, μmol L^{-1}).

Cell Line	TGI (μmol L^{-1})			
	Pd-Sac	**Doxorubicin**	**K$_2$PdCl$_4$**	**Sac**
U251	357.5 ± 51.2	>46	>765	>1500
MCF-7	547.6 ± 5.7	5.2 ± 1.6	>765	>1500
NCI-ADR/RES	>586	>46	>765	>1500
786-0	380 ± 66	3.5 ± 2.0	>765	>1500
NCI-H460	>586	>46	>765	>1500
PC-3	155.6 ± 39.1	1.5 ± 0.6	>765	>1500
OVCAR-3	296.2 ± 116.3	4.6 *	>765	>1500
HT29	269.0 ± 80.8	>46	>765	>1500
K562	231.1 ± 59.0	1.7 ± 0.6	>765	>1500
UACC-62	63.5 ± 9.7	<0.046	n.t.	n.t.
SCC15	570.7 ± 0.3	1.8 ± 0.6	n.t.	n.t.
SCC4	>586	3.5 ± 1.2	n.t.	n.t.
FaDu	460.8 ± 86.3	5.4 ± 2.3	n.t.	n.t.
HaCaT	>586	1.4 ± 0.4	>765	>1500

Human tumorigenic cell lines [glioblastoma (U251), mammary adenocarcinoma (MCF-7), multi-drug-resistant high-grade ovarian serous adenocarcinoma (NCI-ADR/RES), renal cell carcinoma (786-0), large cell lung carcinoma (NCI-H460), adenocarcinoma of prostate (PC-3), high-grade ovarian serous adenocarcinoma (OVCAR-03), rectosigmoid adenocarcinoma (HT-29), chronic myelogenous leukemia (K562), melanoma (UACC-62), squamous cell carcinoma (SCC) of the tongue (SCC4 and SCC15), and SCC of the pharynx (FaDu)]; human non-tumorigenic cell line (HaCaT, immortalized keratinocytes). Concentration range: 0.586–586 μmol L^{-1} (Pd-sac, sac, and K$_2$PdCl$_4$), 0.046–46 μmol L^{-1} (doxorubicin); time exposure = 48 h; n.t. = not tested; * = estimated effective concentration (standard error greater than the calculated effective concentration).

2.3. Determination of Mutagenic Activity

Table 3 shows the mean number of revertants/plate (M), the standard deviation (SD), and the mutagenic index (MI) observed in *Salmonella* Typhimurium strains TA98, TA100, TA102, and TA97a after the treatments with Pd-sac, in the presence (+S9) and absence (−S9) of metabolic activation.

Table 3. Mutagenic activity expressed as the mean and standard deviation of the number of revertants/plate and the mutagenic index (MI) in bacterial strains TA98, TA100, TA102, and TA97a treated with Pd-sac at various doses with (+S9) or without (−S9) metabolic activation.

Treatments		Number of Revertants (M $\pm$ SD)/Plate and MI							
		TA 98		TA 100		TA 102		TA 97a	
		−S9	+S9	−S9	+S9	−S9	+S9	−S9	+S9
	C−	40 ± 5	33 ± 4	119 ± 11	124 ± 13	304 ± 20	342 ± 46	144 ± 18	136 ± 13
	C+ [a]	880 ± 51 **	1410 ± 77 **	1272 ± 102 **	1458 ± 89 **	1547 ± 91 **	1349 ± 133 **	1472 ± 78 **	1160 ± 114 **
	25	$50 \pm 6 (1.24)$	$37 \pm 2 (1.12)$	143 ± 17 (1.20)	144 ± 29 (1.16)	350 ± 17 (1.15)	381 ± 25 (1.12)	158 ± 25 (1.10)	143 ± 16 (1.05)
	50	$47 \pm 1 (1.16)$	$31 \pm 5 (0.94)$	151 ± 22 (1.26)	139 ± 13 (1.12)	373 ± 10 (1.23)	398 ± 37 (1.16)	162 ± 10 (1.13)	148 ± 26 (1.08)
Pd-sac (μg/plate)	100	$50 \pm 7 (1.25)$	$33 \pm 6 (1.00)$	146 ± 16 (1.23)	133 ± 10 (1.07)	375 ± 26 (1.23)	332 ± 30 (0.97)	177 ± 14 (1.23)	129 ± 20 (0.94)
	150	$42 \pm 2 (1.04)$	$34 \pm 1 (1.02)$	133 ± 27 (1.12)	150 ± 8 (1.21)	311 ± 24 (1.02)	275 ± 19 (0.80)	133 ± 18 (0.92)	135 ± 14 (0.99)
	200	$34 \pm 8 (0.85)$	$31 \pm 2 (0.92)$	108 ± 15 (0.90)	104 ± 16 (0.83)	272 ± 38 (0.89)	282 ± 21 (0.83)	106 ± 27 (0.74)	99 ± 19 (0.72)

M $\pm$ SD = mean and standard deviation; C− = negative control (dimethylsulfoxide, 100 μL/plate); C+ = positive control: (a) 4-nitro-O-phenylenediamine (10.0 μg/plate; -S9 TA98 and TA97a), sodium azide (1.25 μg/plate, −S9 TA100), mitomycin (0.5 μg/plate, −S9 TA102), 2-anthramine (1.25 μg/plate, +S9 TA98, TA100, and TA97a), 2-aminofluorene (10.0 μg/plate, +S9 TA102). Metabolic activation = presence (+S9); absence (−S9). Statistical analysis: one-way ANOVA (** $p < 0.01$ compared to negative control group).

Pd-sac did not affect the average number of revertants compared to the negative control group, regardless of sample dose and *S.* Typhimurium strain. Assuming a mutagenic index greater than 2 (IM $\geq$ 2) as an indication of mutagenic activity [28], Pd-sac can be

considered non-mutagenic under the conditions used in this study. These results are of great relevance when considering the safety of the compound in future in vivo tests.

3. Discussion

In the search for new therapeutic options, several metal complexes have been proposed with the aim of overcoming the adverse effects of cisplatin and its analogs [29]. Palladium(II) complexes appear to be an interesting option due to the similarity in coordination modes and the square-planar configuration of the resulting complexes compared to platinum(II) complexes. Among the different ligands already used in palladium(II) complexes, those described as sulfur donors have been evaluated as potential anti-proliferative agents, with a wide variation in results (from inactive to potent inhibition) depending on the in vitro model and the ligand [29]. Deoxyalliin is a water-soluble garlic derivative with promising biological properties, especially as an antioxidant agent [30]. One particular study showed its ability to inhibit the proliferation of A2780 cells with an IC_{50} in the $mmol \cdot L^{-1}$ range. This treatment resulted in G1/S phase arrest and induction of apoptosis. Therefore, the combination of metal ions with deoxyalliin may lead to complexes with distinct biological profiles [31].

Some palladium(II) compounds have been highlighted in a recent review of metal complexes with activity against skin cancers [23]. While less abundant than the studied Pt(II) complexes, the intrinsic higher reactivity of Pd(II) may lead to unique properties that can be explored biologically. In one example, a palladium complex was active against melanoma cells in the $nmol \cdot L^{-1}$ range, also displaying promising activity in animal models (nude mice injected with ME1402 cells) [32].

Curiously enough, all Pd(II) complexes with sulfur donor ligands listed by Jahromi et al. [29] had the metal center coordinated with two sulfur atoms in a *cis* configuration. In the Pd-sac complex, as shown in Figure 2, the sulfur atoms were in a *trans* configuration. This characteristic might influence the anti-proliferative effect of Pd-sac. Different from other water-soluble organic sulfur compounds found in garlic, such as alliin [33,34], deoxyalliin did not affect the proliferation of the evaluated cell lines in this study (Table 2).

Considering compounds containing alliin-like ligands, a recent study by Kahrović and colleagues reported on a series of ruthenium compounds of either L-alliin or L-deoxyalliin, which were evaluated against HeLa (cervical carcinoma), SW620 (colorectal adenocarcinoma, metastatic), MCF-7 (breast adenocarcinoma), CFPAC-1 (ductal pancreatic adenocarcinoma), and HFF-1 (foreskin fibroblasts) cell lines [35]. Two Ru(II) complexes that were obtained were diamagnetic, with an octahedral Ru(II) metal center surrounded by two bidentate alliin molecules and two monodentate solvent molecules, while a Ru(III) compound was paramagnetic with an octahedral central Ru(III) surrounded by five ammonia molecules and one monodentate anionic O-bonded alliin ligand. The compounds were more cytotoxic against the HFF-1 cell line than the cancer cell ones, indicating the absence of anti-proliferative activity. This is in contrast with the results obtained here for the Pd-sac compound, which showed no major cytotoxicity against HaCaT cells. Modest results of the Pd-sac complex against SCC were found in the current study, suggesting that the use of the compound in this type of skin cancer should be limited.

Compared to the Ag-NMS complex recently reported by our group [24], the Pd-sac complex was, in general, less active against cancer cells. However, its water solubility may facilitate its incorporation in formulations. Additionally, the absence of cytotoxic activity against HaCaT keratinocytes and the absence of mutagenic activity encourages further studies to evaluate its potential mechanism of action against melanoma cells. Perspectives also include in vivo studies concerning the topical application of the complex in the treatment of skin cancers.

4. Materials and Methods

4.1. Materials

L-Deoxyalliin ($C_6H_{11}NO_2S$, ≥98%) was purchased from LKT-Labs (St. Paul, MN, USA). Potassium hydroxide, deuterium oxide (D_2O), and lithium tetrachloridopalladate(II) hydrate $Li_2PdCl_4 \cdot nH_2O$, 97% were obtained from Sigma-Aldrich Laboratories (St. Louis, MO, USA). The reagents were used as received. Elemental analyses were performed on a Perkin Elmer 2400 CHNS/O Analyzer (Shelton, CT, USA).

4.2. Synthesis of the Pd(II) Complex

The palladium(II) complex with deoxyalliin was synthesized following the procedure described in the literature [25]. First, deoxyalliin (1.12×10^{-3} mol) was suspended in methanol, and potassium hydroxide (1.12×10^{-3} mol) was added. The reaction was maintained under stirring until solubilization of the ligand. Afterwards, a freshly prepared methanolic solution of Li_2PdCl_4 (5.60×10^{-4} mol) was added to the alkaline deoxyalliin solution and kept at room temperature with stirring for 2 h. A solid pale yellowish complex was slowly precipitated. The complex was collected by filtration, washed with methanol, cooled, and dried in a desiccator under P_4O_{10}. The yield was 64%. Elemental analysis of the powder sample confirmed the 1:2 Pd:sac composition. Anal. Calcd. for $PdC_{12}H_{20}N_2O_4S_2$ (%): C 33.8, H 4.72, N 6.56. Found (%) C 33.5, H 4.48, N 6.52. The ^1H, ^{13}C, and $\{^{15}N,^1H\}$ 2D HMBC NMR spectra were recorded in D_2O, and the results are consistent with previously reported data (for full NMR data interpretation, see the supporting information and Figure S1) [25,26]. Crystals suitable for single-crystal X-ray diffraction studies were obtained by using the liquid–vapor diffusion method, where the complex was first dissolved in water, then acetone was slowly diffused into the solution of the palladium(II) complex.

4.3. Cell Line Culture

In this experiment, thirteen tumorigenic cell lines [glioblastoma (U251), melanoma (UACC-62), mammary adenocarcinoma (MCF-7), multi-drug-resistant high-grade ovarian serous adenocarcinoma (NCI-ADR/RES), renal cell carcinoma (786-0), large cell lung carcinoma (NCI-H460), adenocarcinoma of prostate (PC-3), high-grade ovarian serous adenocarcinoma (OVCAR-03), rectosigmoid adenocarcinoma (HT-29), chronic myelogenous leukemia (K562), squamous cell carcinoma (SCC) of the tongue (SCC4 and SCC15), SCC of the pharynx (FaDu)] and one non-tumorigenic human keratinocyte (HaCaT) cell line were analyzed. The SCC4, SCC15, and HaCaT were provided by the Piracicaba Dental School of the University of Campinas-UNICAMP (Piracicaba, SP, Brazil); the FaDu was provided by the Odontology School of the University of São Paulo-USP (São Paulo, Brazil), while the other human tumor cell lines were provided by the Frederick Cancer Research & Development Center, National Cancer Institute, Frederick, MD, USA. All cell lines were cultivated in complete medium [Roswell Park Memorial Institute (RPMI) 1640, Gibco®, Grand Island, NY, USA], 5% fetal bovine serum (code number 16000, Gibco®, Grand Island, NY, USA), and 1% penicillin–streptomycin mixture (Vitrocell®, Campinas, SP, Brazil; 1000 U·mL^{-1}:1000 mg·mL^{-1}) at 37 °C in 5% CO_2. The experiments were performed with cells at passage 4 to 10 after thawing.

4.4. Experimental Protocol

Each cell line was seeded in 96-well plates (100 μL/well, cell density from 3 to 6×10^3 cells/well) and allowed to recover for 24 h before sample addition in triplicates (100 μL/well, Pd-sac, sac, and palladium(II) salt K_2PdCl_4 0.25 to 250 μg·mL^{-1}) and incubated for 48 h at 37 °C and 5 % CO_2. Doxorubicin (0.025 to 25 μg·mL^{-1}) was used as a positive control. Before (T0) and after (T1) sample addition, cells were fixed with trichloroacetic acid (TCA, 50 %, 50 μL/well), and cell proliferation quantification was determined by the sulforhodamine B (SRB) protocol at 540 nm. Considering the difference between T1 and T0 absorbance values as representing 100 % of cell proliferation, the per-

centage of proliferation of each cell line in the presence of each sample concentration was calculated and plotted as cell growth versus sample concentration (expressed in molarity). Using these curves, the sample concentration required to promote total growth inhibition (TGI) of each cell line was calculated (two independent experiments) by sigmoidal regression using Origin 8.0 software and expressed in μM [36].

4.5. Single-Crystal X-ray Diffraction Data

The single-crystal X-ray diffraction studies of the Pd-sac complex were performed in a Bruker APEX II duo CCD area detector diffractometer (Bruker, Karlsruhe, Germany) using MoKα (λ = 0.71073 Å) radiation from a fine-focus sealed tube with a curved graphite monochromator. Data processing, structure solution and refinement, and computing details are presented in Supporting Information.

The molecular and crystallographic graphs were generated using Mercury (v. 2022.3.0) [37]. The crystallographic data and structural refinement of all compounds are summarized in Table S2. The crystallographic information file was validated by the CheckCIF server and deposited in CSD with the code number 2350462. The CIF file can be obtained free of charge via www.ccdc.cam.ac.uk.

4.6. Determination of Mutagenicity

For the determination of the mutagenic activity of Pd-sac, the Ames test was performed according to the methodology described in the literature [28]. Full details are presented in the Supporting Information.

5. Conclusions

Our study highlights two new aspects of the Pd-sac complex. First, we confirmed the trans configuration of the sac ligands surrounding the Pd(II) metal center by single-crystal X-ray diffraction. This was first hypothesized by us in the past, based on infrared and NMR data in combination with molecular modeling studies. Secondly, the cytotoxic screening demonstrated that the Pd-sac complex exhibits modest but selective anti-proliferative effects over a panel of tumor cells, particularly against UACC-62 melanoma cells. In addition to its water solubility, we also demonstrated here that Pd-sac is non-mutagenic, which is advantageous for the further exploration of this compound in the context of prospective antitumoral drugs.

Supplementary Materials: The following supporting information can be downloaded at: https://www.mdpi.com/article/10.3390/inorganics12070194/s1, Figure S1: (a) ^{1}H NMR spectra and (b) ^{1}H-^{15}N HMBC correlation plot of Pd-sac dissolved in D_2O, Figure S2: Anti-proliferative profile of deoxyalliin (A, sac, 1.5–1500 μM) and K_2PdCl_4 (B, 0.765–765 μM). Human tumor cell lines: glioblastoma (U251), mammary adenocarcinoma (MCF-7), multi-drug-resistant high-grade ovarian serous adenocarcinoma (NCI-ADR/RES), renal cell carcinoma (786-0), large cell lung carcinoma (NCI-H460), adenocarcinoma of prostate (PC-3), high-grade ovarian serous adenocarcinoma (OVCAR-03), rectosigmoid adenocarcinoma (HT-29), chronic myelogenous leukemia (K562). Human non-tumorigenic keratinocytes were HaCaT. These compounds were not evaluated against melanoma (UACC-62), squamous cell carcinoma (SCC) of the tongue (SCC4 and SCC15), and SCC of the pharynx (FaDu). See Table 2 in the main text for calculated TGI values. Figure S3: Anti-proliferative profile of the Pd-sac complex (a,c) and doxorubicin (b,d) against a human cell line panel after 48 h of exposure. (a,b) human cell panel: nine tumorigenic cell lines [glioblastoma (U251), mammary adenocarcinoma (MCF-7), multi-drug-resistant high-grade ovarian serous adenocarcinoma (NCI-ADR/RES), renal cell carcinoma (786-0), large cell lung carcinoma (NCI-H460), adenocarcinoma of prostate (PC-3), high-grade ovarian serous adenocarcinoma (OVCAR-03), rectosigmoid adenocarcinoma (HT-29), and chronic myelogenous leukemia (K562)] and one non-tumorigenic cell line (HaCaT, immortalized keratinocytes); (c,d) human cell panel: four tumorigenic cell lines [melanoma (UACC-62), squamous cell carcinoma (SCC) of the tongue (SCC4 and SCC15), and SCC of the pharynx (FaDu)] and one non-tumorigenic cell line (HaCaT, immortalized keratinocytes). Concentration range: 0.586–586 μmol L^{-1} (a,c), 0.046–46 μmol L^{-1} (b and d). Table S1: Hydrogen-bond geometry for Pd-sac, Table S2: Ex-

perimental details for the Pd-sac crystal structure. References are contained within Supplementary Materials [38–44].

References

1. Medici, S.; Peana, M.; Nurchi, V.M.; Zoroddu, M.A. Medical Uses of Silver: History, Myths, and Scientific Evidence. *J. Med. Chem.* **2019**, *62*, 5923–5943. [CrossRef]
2. Medici, S.; Peana, M.; Crisponi, G.; Nurchi, V.M.; Lachowicz, J.I.; Remelli, M.; Zoroddu, M.A. Silver Coordination Compounds: A New Horizon in Medicine. *Coord. Chem. Rev.* **2016**, *327–328*, 349–359. [CrossRef]
3. Sadler, P.J.; Sue, R.E. The Chemistry of Gold Drugs. *Met.-Based Drugs* **1994**, *1*, 107–144. [CrossRef]
4. Rosenberg, B.; Vancamp, L.; Trosko, J.E.; Mansour, V.H. Platinum Compounds: A New Class of Potent Antitumour Agents. *Nature* **1969**, *222*, 385–386. [CrossRef]
5. Kelland, Lloyd. The Resurgence of Platinum-Based Cancer Chemotherapy. *Nat. Rev. Cancer* **2007**, *7*, 573–584. [CrossRef]
6. Ho, G.Y.; Woodward, N.; Coward, J.I.G. Cisplatin versus Carboplatin: Comparative Review of Therapeutic Management in Solid Malignancies. *Crit. Rev. Oncol./Hematol.* **2016**, *102*, 37–46. [CrossRef]
7. Romani, A.M.P. Cisplatin in Cancer Treatment. *Biochem. Pharmacol.* **2022**, *206*, 115323. [CrossRef] [PubMed]
8. Paprocka, R.; Wiese-Szadkowska, M.; Janciauskiene, S.; Kosmalski, T.; Kulik, M.; Helmin-Basa, A. Latest Developments in Metal Complexes as Anticancer Agents. *Coord. Chem. Rev.* **2022**, *452*, 214307. [CrossRef]
9. Kapdi, A.R.; Fairlamb, I.J.S. Anti-Cancer Palladium Complexes: A Focus on PdX2L2, Palladacycles and Related Complexes. *Chem. Soc. Rev.* **2014**, *43*, 4751–4777. [CrossRef]
10. Alam, M.N.; Huq, F. Comprehensive Review on Tumour Active Palladium Compounds and Structure–Activity Relationships. *Coord. Chem. Rev.* **2016**, *316*, 36–67. [CrossRef]
11. Mjos, K.D.; Orvig, C. Metallodrugs in Medicinal Inorganic Chemistry. *Chem. Rev.* **2014**, *114*, 4540–4563. [CrossRef] [PubMed]
12. Tookad | European Medicines Agency. Available online: https://www.ema.europa.eu/en/medicines/human/EPAR/tookad (accessed on 22 April 2024).
13. Xue, Q.; Zhang, J.; Jiao, J.; Qin, W.; Yang, X. Photodynamic Therapy for Prostate Cancer: Recent Advances, Challenges and Opportunities. *Front. Oncol.* **2022**, *12*, 980239. [CrossRef] [PubMed]
14. Sung, H.; Ferlay, J.; Siegel, R.L.; Laversanne, M.; Soerjomataram, I.; Jemal, A.; Bray, F. Global Cancer Statistics 2020: GLOBOCAN Estimates of Incidence and Mortality Worldwide for 36 Cancers in 185 Countries. *CA A Cancer J Clin.* **2021**, *71*, 209–249. [CrossRef] [PubMed]

15. Robert, C.; Schachter, J.; Long, G.V.; Arance, A.; Grob, J.J.; Mortier, L.; Daud, A.; Carlino, M.S.; McNeil, C.; Lotem, M.; et al. Pembrolizumab versus Ipilimumab in Advanced Melanoma. *N. Engl. J. Med.* **2015**, *372*, 2521–2532. [CrossRef] [PubMed]

16. Robert, C.; Long, G.V.; Brady, B.; Dutriaux, C.; Maio, M.; Mortier, L.; Hassel, J.C.; Rutkowski, P.; McNeil, C.; Kalinka-Warzocha, E.; et al. Nivolumab in Previously Untreated Melanoma without *BRAF* Mutation. *N. Engl. J. Med.* **2015**, *372*, 320–330. [CrossRef] [PubMed]

17. Hu, H.; Li, B.; Wang, J.; Tan, Y.; Xu, M.; Xu, W.; Lu, H. New Advances into Cisplatin Resistance in Head and Neck Squamous Carcinoma: Mechanisms and Therapeutic Aspects. *Biomed. Pharmacother.* **2023**, *163*, 114778. [CrossRef] [PubMed]

18. Cramer, J.D.; Burtness, B.; Le, Q.T.; Ferris, R.L. The Changing Therapeutic Landscape of Head and Neck Cancer. *Nat. Rev. Clin. Oncol.* **2019**, *16*, 669–683. [CrossRef] [PubMed]

19. Ilić, D.R.; Jevtić, V.V.; Radić, G.P.; Arsikin, K.; Ristić, B.; Harhaji-Trajković, L.; Vuković, N.; Sukdolak, S.; Klisurić, O.; Trajković, V.; et al. Synthesis, Characterization and Cytotoxicity of a New Palladium(II) Complex with a Coumarine-Derived Ligand. *Eur. J. Med. Chem.* **2014**, *74*, 502–508. [CrossRef] [PubMed]

20. Pruchnik, H.; Lis, T.; Latocha, M.; Zielińska, A.; Pruchnik, F.P. Palladium(II) Complexes with Tris(2-Carboxyethyl)Phosphine, Structure, Reactions and Cytostatic Activity. *J. Inorg. Biochem.* **2016**, *156*, 14–21. [CrossRef]

21. Da Silva, B.A.O.; Dias, I.S.; Sarto, L.E.; de Gois, E.P.; Torres, C.; de Almeida, E.T.; Gouvêa, C.M.C.P. Cytotoxicity Induced by Newly Synthesized Palladium (II) Complexes Lead to the Death of MCF-7 and MDA-MB-435 Cancer Cell Lines. *Adv. Pharm. Bull.* **2021**, *13*, 160–169. [CrossRef]

22. Sarto, L.E.; Gois, E.P.D.; Andrade, G.G.D.; Almeida, M.S.D.; Freitas, J.T.J.; Júnior, A.D.S.R.; Franco, L.P.; Torres, C.; Almeida, E.T.D.; Gouvêa, C.M.C.P. Anticancer Potential of Palladium(II) Complexes With Schiff Bases Derived from 4-Aminoacetophenone Against Melanoma In Vitro. *Anticancer Res.* **2019**, *39*, 6693–6699. [CrossRef] [PubMed]

23. Manzano, C.M.; Nakahata, D.H.; de Paiva, R.E.F. Revisiting Metallodrugs for the Treatment of Skin Cancers. *Coord. Chem. Rev.* **2022**, *462*, 214506. [CrossRef]

24. Candido, T.Z.; de Paiva, R.E.F.; Figueiredo, M.C.; de Oliveira Coser, L.; Frajácomo, S.C.L.; Abbehausen, C.; Cardinalli, I.A.; Lustri, W.R.; Carvalho, J.E.; Ruiz, A.L.T.G.; et al. Silver Nimesulide Complex in Bacterial Cellulose Membranes as an Innovative Therapeutic Method for Topical Treatment of Skin Squamous Cell Carcinoma. *Pharmaceutics* **2022**, *14*, 462. [CrossRef] [PubMed]

25. Corbi, P.P.; Massabni, A.C.; Moreira, A.G.; Medrano, F.J.; Jasiulionis, M.G.; Costa-Neto, C.M. Synthesis, Characterization, and Biological Activity of a New Palladium(II) Complex with Deoxyalliin. *Can. J. Chem.* **2005**, *83*, 104–109. [CrossRef]

26. Corbi, P.P.; Massabni, A.C. 1H-15N NMR Studies of the Complex Bis(S-Allyl-L-Cysteinate)Palladium(II). *Spectrochim. Acta Part A Mol. Biomol. Spectrosc.* **2006**, *64*, 418–419. [CrossRef] [PubMed]

27. Spera, M.B.M.; Quintão, F.A.; Ferraresi, D.K.D.; Lustri, W.R.; Magalhães, A.; Formiga, A.L.B.; Corbi, P.P. Palladium(II) Complex with S-Allyl-L-Cysteine: New Solid-State NMR Spectroscopic Measurements, Molecular Modeling and Antibacterial Assays. *Spectrochim. Acta Part A Mol. Biomol. Spectrosc.* **2011**, *78*, 313–318. [CrossRef] [PubMed]

28. Cerqueira, I.H.; Mieli, M.J.; Pereira, A.K.; Corbi, P.P.; Resende, F. Evaluation of the Cytotoxicity and Genotoxicological Safety Profile of Bioactive Silver(I) Complexes with Aminoadamantane Ligands. *Quim. Nova* **2024**, *47*, e-20240002. [CrossRef]

29. Jahromi, E.Z.; Divsalar, A.; Saboury, A.A.; Khaleghizadeh, S.; Mansouri-Torshizi, H.; Kostova, I. Palladium Complexes: New Candidates for Anti-Cancer Drugs. *J. Iran. Chem. Soc.* **2016**, *13*, 967–989. [CrossRef]

30. Rais, N.; Ved, A.; Ahmad, R.; Kumar, M.; Deepak Barbhai, M.; Radha; Chandran, D.; Dey, A.; Dhumal, S.; Senapathy, M.; et al. S-Allyl-L-Cysteine—A Garlic Bioactive: Physicochemical Nature, Mechanism, Pharmacokinetics, and Health Promoting Activities. *J. Funct. Foods* **2023**, *107*, 105657. [CrossRef]

31. Xu, Y.; Feng, J.; Zhang, D.; Zhang, B.; Luo, M.; Su, D.; Lin, N. S-Allylcysteine, a Garlic Derivative, Suppresses Proliferation and Induces Apoptosis in Human Ovarian Cancer Cells In Vitro. *Acta Pharmacol. Sin.* **2014**, *35*, 267–274. [CrossRef]

32. Aliwaini, S.; Swarts, A.J.; Blanckenberg, A.; Mapolie, S.; Prince, S. A Novel Binuclear Palladacycle Complex Inhibits Melanoma Growth In Vitro and In Vivo through Apoptosis and Autophagy. *Biochem. Pharmacol.* **2013**, *86*, 1650–1663. [CrossRef] [PubMed]

33. Zhang, H.; Wang, H.; Qin, L.; Lin, S. Garlic-derived Compounds: Epigenetic Modulators and Their Antitumor Effects. *Phytother. Res.* **2024**, *38*, 1329–1344. [CrossRef] [PubMed]

34. Maheshwari, N.; Sharma, M.C. Anticancer Properties of Some Selected Plant Phenolic Compounds: Future Leads for Therapeutic Development. *J. Herb. Med.* **2023**, *42*, 100801. [CrossRef]

35. Zahirović, A.; Žilić, D.; Pavelić, S.K.; Hukić, M.; Muratović, S.; Harej, A.; Kahrović, E. Type of Complex–BSA Binding Forces Affected by Different Coordination Modes of Alliin in Novel Water-Soluble Ruthenium Complexes. *New J. Chem.* **2019**, *43*, 5791–5804. [CrossRef]

36. Monks, A.; Scudiero, D.; Skehan, P.; Shoemaker, R.; Paull, K.; Vistica, D.; Hose, C.; Langley, J.; Cronise, P.; Vaigro-Wolff, A.; et al. Feasibility of a High-Flux Anticancer Drug Screen Using a Diverse Panel of Cultured Human Tumor Cell Lines. *JNCI J. Natl. Cancer Inst.* **1991**, *83*, 757–766. [CrossRef] [PubMed]

37. Macrae, C.F.; Bruno, I.J.; Chisholm, J.A.; Edgington, P.R.; McCabe, P.; Pidcock, E.; Rodriguez-Monge, L.; Taylor, R.; Van De Streek, J.; Wood, P.A. Mercury CSD 2.0—New Features for the Visualization and Investigation of Crystal Structures. *J. Appl. Crystallogr.* **2008**, *41*, 466–470. [CrossRef]

38. Fulmer, G.R.; Miller, A.J.M.; Sherden, N.H.; Gottlieb, H.E.; Nudelman, A.; Stoltz, B.M.; Bercaw, J.E.; Goldberg, K.I. NMR Chemical Shifts of Trace Impurities: Common Laboratory Solvents, Organics, and Gases in Deuterated Solvents Relevant to the Organometallic Chemist. *Organometallics* **2010**, *29*, 2176–2179. [CrossRef]

39.   Bruker. *APEX2, SAINT and SADABS*; Bruker AXS Inc.: Madison, WI, USA, 2010.

40.   Sheldrick, G.M. A Short History of SHELX. *Acta Cryst. A* **2008**, *64*, 112–122. [CrossRef]

41.   Sheldrick, G.M. Crystal Structure Refinement with SHELXL. *Acta Crystallogr. C Struct. Chem.* **2015**, *71*, 3–8. [CrossRef]

42.   Maron, D.M.; Ames, B.N. Revised Methods for the Salmonella Mutagenicity Test. *Mutat. Res./Environ. Mutagen. Relat. Subj.* **1983**, *113*, 173–215. [CrossRef]

43.   Bernstein, L.; Kaldor, J.; McCann, J.; Pike, M.C. An Empirical Approach to the Statistical Analysis of Mutagenesis Data from the Salmonella Test. *Mutat. Res./Environ. Mutagen. Relat. Subj.* **1982**, *97*, 267–281. [CrossRef] [PubMed]

44.   Mortelmans, K.; Zeiger, E. The Ames *Salmonella*/Microsome Mutagenicity Assay. *Mutat. Res./Fundam. Mol. Mech. Mutagen.* **2000**, *455*, 29–60. [CrossRef] [PubMed]